Nagahara M,et.al	Correlated expression of CD47 and SIRP1 in bone marrow and in peripheral blood predicts recurrence in breast cancer patients	***Clin Cancer Res***	16(18)	4625-4635	2010
Yokobori T,et.al	Clinical significance of Stanniocalcin 2 as a prognostic marker in gastric cancer	***Ann Surg Oncol***	17(10)	2601-2607	2010
Nagai K,et.al	Long-term culture following ES-like gene-induced reprogramming elicits an aggressive phenotype in mutated cholangiocellular carcinoma cells	***Biochem Biophys Res Commun***	395	258-263	2010
Iwatsuki, M,et.al	Loss of FBXW7, a cell cycle regulating gene, in colorectal cancer: Clinical significance	***Int J Cancer***	126	1828-1837	2010
Hirose H. et.al	Notch pathway as candidate therapeutic target in Her2/Neu/ErbB2 receptor-negative breast tumors	***Oncology Reports***	23	35-43	2010

Biochemical and Biophysical Research Communications 395 (2010) 258–263

Contents lists available at ScienceDirect

Biochemical and Biophysical Research Communications

journal homepage: www.elsevier.com/locate/ybbrc

Long-term culture following ES-like gene-induced reprogramming elicits an aggressive phenotype in mutated cholangiocellular carcinoma cells

Ken-ichi Nagai [a], Hideshi Ishii [a,b,*], Norikatsu Miyoshi [a], Hiromitsu Hoshino [a], Toshiyuki Saito [c], Tetsuya Sato [b], Yoshito Tomimaru [a], Shogo Kobayashi [a], Hiroaki Nagano [a], Mitsugu Sekimoto [a], Yuichiro Doki [a], Masaki Mori [a,b,**]

[a] Department of Gastroenterological Surgery, Osaka University Graduate School of Medicine, Yamadaoka 2-2, Suita, Osaka 565-0871, Japan
[b] Department of Molecular and Cellular Biology, Division of Molecular and Surgical Oncology, Kyushu University, Medical Institute of Bioregulation, Tsurumihara 4546, Beppu, Ohita 874-0838, Japan
[c] Transcriptome Profiling Group, National Institute of Radiological Sciences, Research Center for Charged Particle Therapy, Inage-Anagawa 4-9-1, Chiba 263-8555, Japan

ARTICLE INFO

Article history:
Received 17 March 2010
Available online 7 April 2010

Keywords:
Cholangiocelluar carcinoma
Malignancy
Reprogramming
Induced pluripotent cancer
Cancer stem cells

ABSTRACT

Background: We recently reported that gastrointestinal (GI) cancer cells can be reprogrammed to a pluripotent state by the ectopic expression of defined embryonic stem (ES)-like transcriptional factors. The induced pluripotent cancer (iPC) cells from GI cancer were sensitized to chemotherapeutic agents and differentiation-inducing treatment during a short-term culture, although a phenotype induced by long-term culture needs to be studied.

Methods: A long-term cultured (Lc)-iPC cells were produced in GI cancer cell lines by virus-mediated introduction of four ES-like genes-*c-MYC*, *SOX2*, *OCT3/4*, and *KLF4*-followed by a culture more than three months after iPC cells induction. An acquired state was studied by expression of immature-related surface antigens, Tra-1-60, Tra-1-81, Tra-2-49, and Ssea-4; and epigenetic trimethyl modification at lysine 4 of histone H3. Sensitivity to chemotherapeutic agents and tumorigenicity were studied in Lc-iPC cells.

Results: Whereas the introduction of defined factors of iPC cells once induced an immature state and sensitized cells to therapeutic reagents, the endogenous expression of the ES-like genes except for activated endogenous *c-MYC* was down-regulated in a long-term culture, suggesting a high magnitude of the reprogramming induction by defined factors and the requirement of therapeutic maintenance in Lc-iPC cells from cholangiocellular carcinoma HuCC-T1 cells, which harbor $TP53^{R175H}$ and $KRAS^{G12D}$. The Lc-iPC cells showed resistance to 5-fluorouracil in culture, and high tumorigenic ability with activated endogenous *c-MYC* in immunodeficient mice.

Conclusion: The Lc-iPC cells from HuCC-T1 might be prone to an undesirable therapeutic response because of an association with the activated endogenous *c-MYC*. To consider the possible therapeutic approach in GI cancer, it would be necessary to develop a predictive method for evaluating the improper reprogramming-associated aggressive phenotype of iPC cells.

1. Introduction

Cancer is a genetic and epigenetic disorder [1] characterized by abnormal differentiation of cells [2]. Although genetic alterations, including activation of tumor-promoting oncogenes and inactivation of growth constraint tumor suppressor genes, are involved in stepwise carcinogenesis, abnormal epigenetic modifications, which are irrelevant to genetic codes, are undoubtedly important for generating malignant cancer cell phenotypes. Nevertheless, the magnitude of effect of epigenetic corrections remains to be understood.

Non-cancerous somatic cells have recently been reprogrammed to a pluripotent state (induced pluripotent stem [iPS] cells) by the ectopic expression of defined embryonic stem (ES)-like transcriptional factors, *c-MYC*, *SOX2*, *OCT3/4*, and *KLF4* [3]. We have shown that introducing defined factors induced pluripotent cancer (iPC) cells from human gastrointestinal (GI) cancer [4]. The iPC cells were sensitized to chemotherapeutic agents and differentiation-inducing treatment, and tumorigenicity was reduced after a short-term culture. While the defined factor-induced reprogramming occurs fundamentally at the epigenetic level [5], the study

* Corresponding author at: Department of Gastroenterological Surgery, Osaka University Graduate School of Medicine, Yamadaoka 2-2, Suita, Osaka 565-0871, Japan. Fax: +81 6 6879 3259.
** Corresponding author at: Department of Gastroenterological Surgery, Osaka University Graduate School of Medicine, Yamadaoka 2-2, Suita, Osaka 565-0871, Japan. Fax: +81 6 6879 3259.
E-mail address: mmori@gesurg.med.osaka-u.ac.jp (M. Mori).

0006-291X/$ - see front matter © 2010 Elsevier Inc. All rights reserved.
doi:10.1016/j.bbrc.2010.03.176

indicates the possibility that epigenetic modifications could generate a significant magnitude to induce the sensitivity to differentiation induction and chemotherapy reagents in GI cancer. Nevertheless, long-term behavior of iPC cells with deleterious mutations remains to be studied. Furthermore, safety issues involved in synthesizing tumor-producing iPS cells from non-cancerous somatic cells should be addressed to avoid an unexpected malignant transformation in the course of medical innervations in human diseases.

In the present study, we introduced defined factors in three GI cancer cell lines to establish short-term cultured (Sc)-iPC cells, similar to iPS/iPC cells production [3,4], which were cultured to assess long-term cultured (Lc)-iPC cells. The aggressive phenotype was observed in a cell line with genetic mutations, which were associated with endogenous *c-MYC* activation.

2. Materials and methods

For detailed information see Supplementary Information.

2.1. Cell culture

Three GI cell lines were maintained in DMEM (Sigma, St. Louis, MO) containing 10% fetal bovine serum (FBS) at 37 °C in a 5% humidified CO_2 atmosphere, and used for reprogramming. Colorectal cancer DLD-1 and hepatocellular carcinoma PLC/PRF/5 (PLC) cells were purchased from the Japanese Cancer Research Resources Bank (Tokyo, Japan), and cholangiocellular carcinoma HuCC-T1 cells were a gift from Dr. Gregory J. Gores. PLAT-E cells (Cell Biolabs, San Diego, CA) were maintained in DMEM containing 10% FBS, 1 μg/ml puromycin (Sigma), and 10 μg/ml blasticidin (Sigma). 293FT (Invitrogen, Carlsbad, CA) cells were maintained in DMEM containing 10% FBS and 500 μg/ml geneticin (Invitrogen). The medium was replaced every 2 or 3 days.

2.2. Transfection and Sc-iPC cells production

293FT cells were used to produce the lentiviral vector harboring the mouse retroviral receptor by introducing the pLenti6/UbC/mSlc7a1 plasmid (Addgene Cambridge, MA). After transfection, the lentivirus was purified by filtration. Cancer cells transfected using the lentivirus mSlc7a1, as described above, were infected with retroviruses in the medium. Retroviral vectors were produced by transfecting constructed plasmids into PLAT-E cells, and the culture medium was purified by filtration, concentrated, and used for infection.

Eight days after transduction, the transfected cells in 10% FBS–DMEM were harvested and re-plated on culture plates coated with Matrigel hESC-qualified Matrix (BD Biosciences, Bedford, MA). The medium was replaced the next day with mTeSR1 medium (Stem-Cell Technologies, Vancouver, BC, Canada). Post-Sc-iPC production was induced as described previously [4]. Post-Sc-iPC cells were cultured for an additional 10 weeks in 10% FBS–DMEM primary culture medium until day 90 to induce Lc-iPC cells.

2.3. Quantitative reverse transcription (RT)-PCR

Total RNA was extracted, reverse transcribed, and subjected to quantitative real-time RT-PCR using the LightCycler TaqMan Master kit (Roche Diagnostics GmbH, Mannheim, Germany) and the LightCycler FastStart DNA Master SYBR Green I kit (Roche).

2.4. Immunofluorescence staining

Cells were fixed in 4% paraformaldehyde, immunostained with specific antibodies, and visualized by fluorescence microscopy (BZ-8000; Keyence, Osaka, Japan). For adipogenic or osteogenic differentiation, iPC cells were treated with the supplements (R&D Systems, Minneapolis, MN) in culture medium for 2 weeks.

2.5. Chromatin immunoprecipitation assay

Cells were cross-linked with 1% formaldehyde, immunoprecipitated using the anti-trimethyl lysine 4 histone H3 antibody (Nippon Gene, Toyama, Japan), and used for semi-quantitative PCR.

2.6. Invasion and chemosensitivity assay

Cell invasion was assessed using a CytoSelect Cell Invasion Assay kit (Cell Biolabs) with or without 100 nM retinol (RA; Sigma) or 10 nM 1,25-dihydroxy-vitamin D3 (VD3; Sigma) treatment. The *in vitro* chemotherapeutic sensitivity to 5-fluorouracil (5-FU; Kyowa Hakkou, Tokyo, Japan) was assessed by the 3-(4-,5-dimethylthiazol-2-yl)-2,5-diphenyltetrazolium bromide (MTT; Sigma) assay.

2.7. In vivo tumorigenicity assay

In vivo tumorigenicity was evaluated by transplanting cells into immunodeficient NOD.CB17-Prkdcscid/J (NOD-scid) mice (Charles Liver, Yokohama, Japan). Eight weeks after injection, tumors were dissected, measured, and fixed with 4% paraformaldehyde. Paraffin-embedded tissue was sliced, stained with hematoxylin–eosin (HE), and subjected to immunohistochemistry using the anti-c-Myc antibody.

3. Results

3.1. Introduction of defined ES-like transcriptional factors elicited an immature state in cancer cells

The experimental schedule is shown in Fig. 1A. Four defined factors, *c-MYC*, *SOX2*, *OCT3/4*, and *KLF4*, were transfected into three cancer cell lines, HuCC-T1, PLC, and DLD-1, using the retroviral packaging cell line PLAT-E at day 0. Cells were trypsinized, harvested, and re-plated onto Matrigel-coated plates at day 8 after transfection. The next day, culture dishes were replaced with human ES cell culture medium (mTeSR1). Three weeks after transduction, round-shaped, colonies, which were distinct from background cells, started appearing. The colonies were picked up at day 30 (Supplementary Fig. S1) and *NANOG* expression was confirmed using fluorescence microscopic observation for green fluorescent protein (*Gfp*) expression after transiently transfecting the *NANOG* promoter-*Gfp* vector (data not shown). We obtained approximately ~10 *Gfp*-positive Sc-iPC colonies from 1×10^4 cancer cells.

Quantitative RT-PCR analysis with specific primers showed that a temporal increase in the expression of four transfected genes (Tgs), *c-MYC*, *SOX2*, *OCT3/4*, and *KLF4*, was observed at day 5, although they were absent at day 0. The expression decreased to low or undetectable levels on day 30, suggesting gene silencing (Fig. 1B). In contrast, the transfected and endogenous expression levels of ES-like genes, *c-MYC*, *SOX2*, *OCT3/4*, *KLF4*, *NANOG*, and *REX1*, apparently increased at day 30, compared with those at day 0 (Fig. 1C). The Sc-iPC cells data were consistent with previous findings on non-cancerous somatic cells (iPS cells; [3]) and other cancer cells (iPC cells; [4]).

3.2. Sc-iPC cells expressed immature-related surface antigens and associated epigenetic modifications

To assess the acquisition of an immature state, Sc-iPC cells at day 30 were stained with immature-related surface antigens.

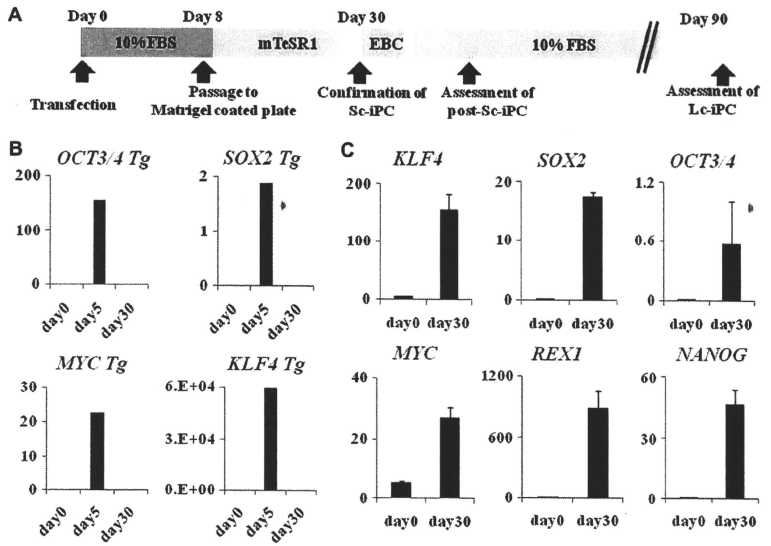

Fig. 1. Induction of ES-like genes in human GI cancer cells. Lentiviral and retroviral-mediated ES-like gene transfer induced a pluripotent state in three GI cancer cell lines to form iPC cells from three GI cancer cell lines. (A) Time course schedule of Sc-iPC, post-Sc-iPC, and Lc-iPC cells production. (B,C) Quantitative RT-PCR of Tg (B) and total mRNA (C) demonstrated temporal transgene expression after transfection and expressed undifferentiated ES-like genes *c-MYC*, *SOX2*, *OCT3/4*, *KLF4*, *NANOG*, and *REX1* in Sc-iPC cells from HuCC-T1 cells. The expression of mRNA copies was normalized against *GAPDH* mRNA expression.

Immunocytochemistry revealed that induced cells were positively stained with tumor-related antigens (Tra)-1-60, Tra-1-81, Tra-2-49, and stage-specific embryonic antigen (Ssea)-4 (Fig. 2A), indicating the maintenance of an immature state in Sc-iPC cells. Similar data were obtained for all three cell lines, and a representative result from HuCC-T1 and PLC cells are shown.

Epigenetic modifications were confirmed by assessing histone methylation. Chromatin immunoprecipitation using the trimethyl histone H3 protein at lysine 4 (H3K4) antibody indicated that H3K4 of *NANOG* and *OCT3/4* promoters were trimethylated in Sc-iPC cells, but not in parent nor post-Sc-iPC cells; post-Sc-iPC cells were prepared from Sc-iPC cells by culturing cells in embryonic body culture conditions (EBC) for 1 week and then in primary culture medium for another 1 week (Fig. 2B). Trimethylation of the *SOX2* promoter was detected in Sc-iPC cells and to a lesser extent in parental cells. The results indicated that the promoters of ES-like genes were activated in Sc-iPC cells.

3.3. Sc-iPC cells showed differentiation in vitro

To assess their ability to differentiate, we placed Sc-iPC cells in differentiation culture medium with an osteogenic or adipogenic supplement for 2 weeks (Fig. 2C and E). The data indicated that Sc-iPC cells were susceptible to differentiation, which was studied by positive staining for Osteocalcin (specific for osteocytes) or Fabp4 (specific for adipose cells), but not for parental cells (Fig. 2D and F; data not shown). Quantitative RT-PCR analysis with specific primers showed that post-Sc-iPC cells from HuCC-T1 were expressing paired box 6 (*PAX6*, representing ectoderm), microtubule-associated protein 2 (*MAP2*, representing ectoderm) and E-cadherin (*CDH1*, representing endoderm). Taken together, it is suggested that Sc-iPC cells have ability to express differentiation markers into three germ layers.

3.4. Sc-iPC cells were sensitized to differentiation-inducing reagents

The proliferation of Sc-iPC (Supplementary Fig. S2A) after 48 h incubation was not significantly different from that of parental HuCC-T1 cells. In contrast, treatment with differentiation inducers of RA or VD3 for 48 h resulted in a significant decrease in the invasiveness ratio of post-Sc-iPC cells compared to HuCC-T1 parental cells (Supplementary Fig. S2B and C). RA is commonly used for the treatment of acute promyelocytic leukemia, which involves differentiation of immature leukemic promyelocytes into mature granulocytes [6]. It has been suggested that RA or VD3 treatment is effective for inducing differentiation of post-Sc-iPC cells.

3.5. Cultured Lc-iPC cells showed increased proliferation and 5-FU resistance

In proliferation assay, Lc-iPC cells from HuCC-T1 proliferated in a high magnitude, compared with parental cells significantly (Fig. 3A). To compare the sensitivity of Lc-iPC cells to anti-cancer drugs with that of parental cells, we performed the MTT assay for 5-FU. The IC_{50} value of Lc-iPC cells from HuCC-T1 cells was significantly higher than that of parental cells (Fig. 3B), indicating that a long-term culture may elicit malignant transformation of iPC cells compared to clones immediately after inducing reprogramming [4].

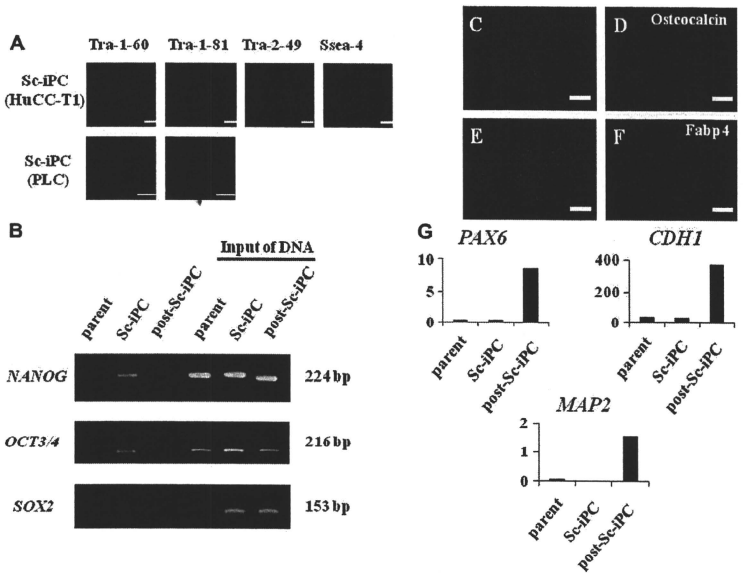

Fig. 2. An immature state and multi-differentiation potential of Sc-iPC cells. (A) Immature-related surface antigens in Sc-iPC cells from HuCC-T1 and PLC were analyzed; Tra-1-60, Tra-1-80, Tra-2-49, and Ssea-4. Bar, 200 μm; Original magnification, 200×. (B) Histone modification status in parental, Sc-iPC, and post-Sc-iPC cells from HuCC-T1 was analyzed using chromatin immunoprecipitation with the trimethyl-K4 H3 antibody. H3 lysine 4 was methylated in the promoter regions for *NANOG* and *OCT3/4* in Sc-iPC cells, but not in parental and post-Sc-iPC cells. Respective sheared chromatin samples were used as control for semi-quantitative PCR. Lineage-directed differentiation of Sc-iPC cells to osteocytes or adipocytes demonstrated that osteocyte-differentiated Sc-iPC cells (C) were positive for Osteocalcin (D) and adipocyte-differentiated Sc-iPC cells (E) were positive for Fabp4 (F). Bar, 200 μm; Original magnification, 100×. (G) *PAX6*, *CDH1*, and *MAP2* expressions were evaluated by quantitative RT-PCR in parental HuCC-T1, Sc-iPC, and post-Sc-iPC cells. The expression of mRNA copies was normalized against *GAPDH* mRNA expression.

3.6. Lc-iPC cells formed c-Myc-positive tumors in immunodeficient mice

Since the preceding proliferation assay indicated high activity, we inoculated HuCC-T1-derived Lc-iPC cells into NOD-scid mice to assess the *in vivo* tumorigenicity. Tumors were formed 4 weeks after inoculation (Fig. 3C and D). Interestingly, 8 weeks after injection the size of these tumors was significantly larger in Lc-iPC cells as compared to that in parental cells (Fig. 3E). The H-E staining indicated that tumors of Lc-iPC cells showed no apparent teratomas, but indicated the presence of a proliferating phenotype as compared to those of parental cells (Fig. 3F and G). Immunohistochemical staining with anti-c-Myc antibody indicated that Lc-iPC-formed tumors were positive for c-Myc, compared to parental cell-derived tumors (Fig. 3H and I), suggesting that c-Myc activation may play a role, at least partially, in the development of a malignant Lc-iPC cell phenotype.

3.7. Lc-iPC cells expressed the activated endogenous c-MYC gene but not other ES-like transcriptional factors

To elucidate the mechanism of activated *c-MYC* expression in Ls-iPC cell-derived tumor in NOD-scid mice, the expressions of endogenous and transgenic ES-like transcriptional factors were investigated in Lc-iPC cells from HuCC-T1. As shown in Fig. 4A, the expression of the ES-like transcriptional factor mRNAs including *SOX2, OCT3/4, KLF4, and NANOG* was decreased drastically, whereas total amount of *c-MYC* expression was detectable in an appreciable level. The origin of *c-MYC* was found to be endogenous, since transgenic *c-MYC* expression was undetected (Fig. 4B), indicating endogenous *c-MYC* activation of Lc-iPC cells increased tumorigenisity in NOD-scid mice.

3.8. Lc-iPC cells lost the expression of immature-related surface antigens and associated epigenetic modifications

To elucidate the immature status of Lc-iPC cells from HuCC-T1, we investigated immature-related surface antigens and histone modification status. Lc-iPC cells from HuCC-T1 lost their expression of immature-related surface antigens including Tra-1-60, Tra-1-81, Tra-2-49, and Ssea-4 (Supplementary Fig. S3); *NANOG, OCT3/4,* and *SOX2* promoters of Lc-iPC cells were slightly trimethylated, indicating that these three ES-like genes were inactivated (Fig. 4C), and suggesting that *c-MYC* is prone to activation in the Lc-iPC cells.

4. Discussion

GI cancer is a major cause of death in several developed countries, including Japan. After therapeutic interventions, such

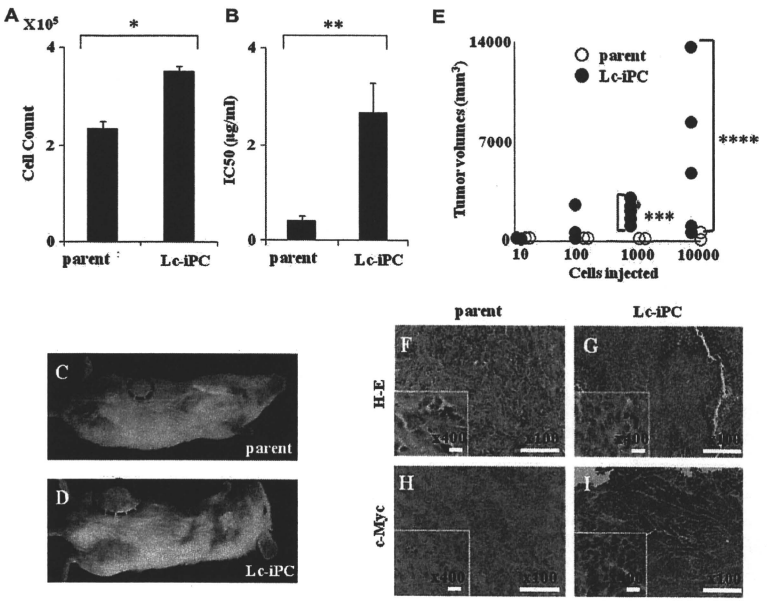

Fig. 3. MTT assay, proliferation *in vitro*, tumor formation *in vivo*, and c-Myc immunohistochemistry by induced Lc-iPC cells from HuCC-T1. Proliferation assay showed an increased proliferation (A; $n = 5$, $^{*}p = 0.012$) and MTT assay showed an increased IC_{50} for 5-FU (B; $n = 7$, $^{**}p = 0.001$) in Lc-iPC cells from HuCC-T1 as compared with parental cells. Lc-iPC and parental cells from HuCC-T1 were subcutaneously transplanted into three parts of NOD-scid mice. Four weeks after injection (C and D), tumors were palpable subcutaneously. Tumors were dissected and measured 8 weeks after injection. Tumors from Lc-iPC cells were larger than those from parental cells when 1000 and 10,000 cells were injected ($n = 6$, $^{***}p = 0.005$, $^{****}p = 0.005$, respectively). H–E staining of dissected tumor, (F) parental cells from HuCC-T1; (G) Lc-iPC cells from HuCC-T1. Tumors from Lc-iPC cells were less differentiated than parental cells. c-Myc immunohistochemistry showed that tumors of Lc-iPC cells from HuCC-T1 (I) expressed c-Myc protein more than those from parental cells (H). Bar, 100 μm; Original magnification, 100×, 400×.

as surgery and conventional chemoradiation therapy, tumor reduction and remission occur in more than half of the cases, although tumors can relapse and spread to other organs, i.e., metastasis. To overcome resistance to therapy, we recently showed that GI cancer reprogramming can sensitize cancer cells to differentiation and chemotherapeutic agents [4], indicating that further investigation is required on reprogramming of cancer cells to discover novel therapeutic approaches.

Several studies have reported reprogramming of cancer cells, including skin cancer or melanoma cells, using vectors harboring micro RNA-302 [7], *OCT3/4*, *c-MYC*, and *KLF4* [8], by nuclear transplantation [9]; but also GI cancer by introducing ES-like genes, which have been mentioned as iPS genes [4]. Introducing defined factors could be the advancement for science and technology as compared with reprogramming by nuclear transplantation, which might be necessary for determining safety issues. iPS cells, similar to ES cells, have the potential to form teratomas following inoculation in immunodeficient mice, presumably through the involvement of retroviral integration, retaining immature clones, and oncogenic *c-MYC* activation, which is consistent with the findings of the present study.

However, the involvement of *c-MYC* should be further investigated. A previous report indicated that tumors formed in iPS cell-derived chimeric mice could be attributed to the reactivation of the *c-MYC* retroviral transgene [10], whereas another report stated that the propensity for teratoma formation from a secondary neurosphere, derived from mice iPS cells, may depend on the tissue of origin but not on *c-MYC* transgene reactivation [11]. In our study, induced Lc-iPC cells showed increased proliferation and chemoresistance to 5-FU and stained strongly positive for c-Myc, which may be relevant to endogenous c-Myc activation in tumors, as detected by quantitative RT-PCR (Fig. 4A and B).

Nevertheless, we must consider other factors involved in iPC cells induction, such as genomic abnormalities, which are the usual characteristics of cancer cells. A possibility is that $TP53^{R175H}$ and $KRAS^{G12D}$ genomic mutations of HuCC-T1 may be relevant to the present observation [13] (data not shown). $KRAS^{G12D}$, a common mutation in solid cancers, is an active form of the *KRAS* gene. Mice expressing oncogenic $Kras^{G12D}$ and mutant *Tp53* accelerated the onset of cancer [12]. Taken together, data suggest that HuCC-T1 reprogramming may affect the pathways of these two mutated proteins.

Based on our results, we are confident of developing more effective differentiation therapies to conquer cancer if we find more appropriate differentiation pathways; however, further analysis of Sc-iPC and Lc-iPC cell properties is needed. Our data suggest that this new reprogramming technology will be a key to conquer bile duct carcinoma through its high magnitude of effect on sensitiza-

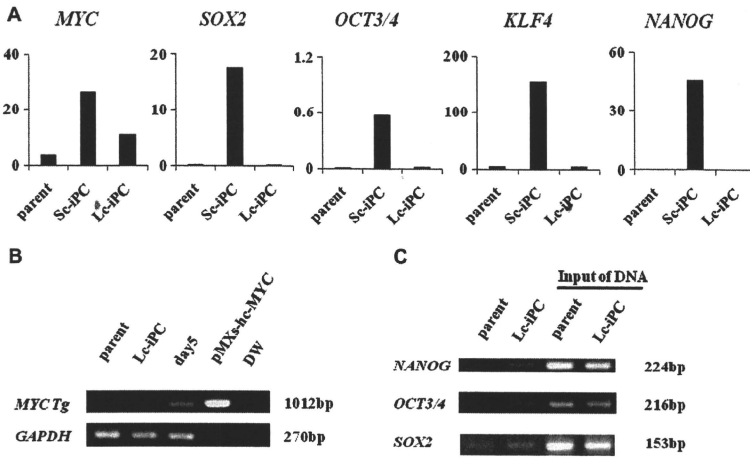

Fig. 4. Immature state of induced Lc-iPC cells from HuCC-T1. (A) Quantitative RT-PCR of total mRNAs of ES-like genes demonstrated genes expression, including *c-MYC*, *SOX2*, *OCT3/4*, *KLF4*, and *NANOG*, of Lc-iPC cells from HuCC-T1, decreased drastically compared to that of Sc-iPC cells except *c-MYC*. The expression of mRNA copies was normalized against *GAPDH* mRNA expression. (B) The RT-PCR of Lc-iPC from HuCC-T1 did not detect transgene (*Tg*) *c-MYC*. Day5, HuCC-T1 cells five days after transfection (*c-MYC*, *SOX2*, *OCT3/4*, and *KLF4*); pMXs-hc-MYC, positive control reaction of vector; DW, negative control with water. (C) Histone modification status in parental and Lc-iPC cells from HuCC-T1 was analyzed using chromatin immunoprecipitation with anti-trimethyl-K4 H3 antibody. The methylation signal at H3 lysine 4 was detected slightly in *NANOG*, *OCT3/4* and *SOX2* promoters in Lc-iPC cells, and *SOX2* in parental cells.

tion to a series of reprogramming-mediated, anti-cancer therapies, and that a predictive method will be necessary for evaluating the improper reprogramming-associated aggressive phenotype of iPC cells. In future, a day will come when cancer will be cured more effectively by newly discovered pharmacogenomic medicine based on reprogramming technology.

5. Conclusion

Although defined factor-induced reprogramming of gastrointestinal cancer cells is a promising approach for the treatment of cancer, we noted that Lc-iPC cells may be prone to genomic instability presumably due to genetic and epigenetic alterations including endogenous *c-MYC* activation, which is characteristic of cancer cells and is associated with reprogramming technology. To exclude therapy-resistant clones in GI cancer, it is necessary to develop a predictive method for evaluating improper reprogramming-associated aggressive phenotype of reprogrammed cells.

Acknowledgments

We thank Dr. Gregory J. Gores, Mayo Clinic College of Medicine, Rochester, MN, for providing cholangiocellular carcinoma HuCC-T1 cells and Kimie Kitagawa for excellent technical assistance. This work was supported in part by a Grant-in-Aid for Scientific Research on Priority Areas (20012039), a Grant-in-Aid for Scientific Research (S, 21229015; C, 20590313), and a Grant-in-Aid for Young Scientists (B, 21791287) from the Ministry of Education, Culture, Sports, Science, and Technology, Japan; the Kobayashi Foundation for Cancer Research and the Uehara Memorial Foundation, Japan.

Appendix A. Supplementary data

Supplementary data associated with this article can be found, in the online version, at doi:10.1016/j.bbrc.2010.03.176.

References

[1] A.P. Feinberg, R. Ohlsson, S. Henikoff, The epigenetic progenitor origin of human cancer, Nat. Rev. Genet. 7 (2006) 21–33.
[2] T. Reya, S.J. Morrison, M.F. Clarke, et al., Stem cells, cancer, and cancer stem cells, Nature 414 (2001) 105–111.
[3] K. Takahashi, K. Tanabe, M. Ohnuki, et al., Induction of pluripotent stem cells from adult human fibroblasts by defined factors, Cell 131 (2007) 861–872.
[4] N. Miyoshi, H. Ishii, K. Nagai, et al., Defined factors induce reprogramming of gastrointestinal cancer cells, PNAS 107 (2010) 40–45.
[5] S. Yamanaka, Elite and stochastic models for induced pluripotent stem cell generation, Nature 460 (2009) 49–52.
[6] A. Kakizuka, W.H. Miller Jr., K. Umesono, et al., Chromosomal translocation t(15;17) in human acute promyelocytic leukemia fuses RAR alpha with a novel putative transcription factor, PML, Cell 66 (1991) 663–674.
[7] S.L. Lin, D.C. Chang, S. Chang-Lin, et al., Mir-302 reprograms human skin cancer cells into a pluripotent ES-cell-like state, RNA 14 (2008) 2115–2124.
[8] J. Utikal, N. Maherali, W. Kulalert, et al., Sox2 is dispensable for the reprogramming of melanocytes and melanoma cells into induced pluripotent stem cells, J. Cell Sci. 122 (2009) 3502–3510.
[9] K. Hochedlinger, R. Blelloch, C. Brennan, et al., Reprogramming of a melanoma genome by nuclear transplantation, Genes Dev. 18 (2004) 1875–1885.
[10] K. Okita, T. Ichisaka, S. Yamanaka, Generation of germline-competent induced pluripotent stem cells, Nature 448 (2007) 313–317.
[11] K. Miura, Y. Okada, T. Aoi, et al., Variation in the safety of induced pluripotent stem cell lines, Nat. Biotechnol. 27 (2009) 743–745.
[12] L. Johnson, K. Mercer, D. Greenbaum, et al., Somatic activation of the K-ras oncogene causes early onset lung cancer in mice, Nature 410 (2001) 1111–1116.

Web reference

[13] Available from: http://www.sanger.ac.uk, last accessed date, July 15, 2009.

Review Article | DOI 10.3349/ymj.2010.51.5.617 pISSN: 0513-5796, eISSN: 1976-2437 | Yonsei Med J 51(5):617-621, 2010 | YMJ

Perspective beyond Cancer Genomics: Bioenergetics of Cancer Stem Cells

Hideshi Ishii, Yuichiro Doki, and Masaki Mori
Department of Gastroenterological Surgery, Osaka University Graduate School of Medicine, Osaka, Japan.

Received: January 5, 2010
Corresponding author: Dr. Masaki Mori, Department of Gastroenterological Surgery, Osaka University Graduate School of Medicine, Suita, Yamadaoka 2-2, Osaka 565-0871, Japan.
Tel: 81-(0)6-6879-3251, Fax: 81-(0)6-6879-3259
E-mail: mmori@gesurg.med.osaka-u.ac.jp

· The authors have no financial conflicts of interest.

Although the notion that cancer is a disease caused by genetic and epigenetic alterations is now widely accepted, perhaps more emphasis has been given to the fact that cancer is a genetic disease. It should be noted that in the post-genome sequencing project period of the 21st century, the underlined phenomenon nevertheless could not be discarded towards the complete control of cancer disaster as the whole strategy, and in depth investigation of the factors associated with tumorigenesis is required for achieving it. Otto Warburg has won a Nobel Prize in 1931 for the discovery of tumor bioenergetics, which is now commonly used as the basis of positron emission tomography (PET), a highly sensitive noninvasive technique used in cancer diagnosis. Furthermore, the importance of the cancer stem cell (CSC) hypothesis in therapy-related resistance and metastasis has been recognized during the past 2 decades. Accumulating evidence suggests that tumor bioenergetics plays a critical role in CSC regulation; this finding has opened up a new era of cancer medicine, which goes beyond cancer genomics.

Key Words: Cancer, genetics, bioenergetics, cancer stem cells

INTRODUCTION

According to the modern understanding of cancer, it is a disease that is primarily associated with genetic and epigenetic alterations.[1] Numerous studies, including our earlier works, have supported the notion that carcinogenesis involves the activation of tumor-promoting oncogenes and the inactivation of growth-inhibiting tumor suppressor genes. However, extensive research is warranted in two areas, namely, tumor bioenergetics and the cancer stem cell (CSC) hypothesis, which did not receive the required attention after the success of the genome sequencing project ofthe 21st century. An investigation of these two concepts would give rise to a new era in the study of cancer biology. Indeed, recent studies have indicated that the two apparently distinct fields might be related to each other and can converge more rapidly than previously recognized.

TUMOR BIOENERGETICS

The Warburg effect

Otto Warburg won a Nobel Prize in 1931 for his work on respiratory impairment in cancer. Warburg showed that unlike normal tissues that derive most of their

ATP by metabolizing glucose to carbon dioxide and water, which is an oxygen-dependent process performed by the mitochondria, cancer cells rarely depend on mitochondria for respiration and obtain almost half of their ATP by directly metabolizing glucose to lactic acid, even in the presence of oxygen.[2] However, with the discovery that tumors do not show any shift to glycolysis,[3] Warburg's cancer theory (high lactate production and low mitochondrial respiration in tumor under normal oxygen pressure) was gradually discredited. The ascendancy of molecular biology over the last quarter of the century has placed more emphasis on the genetic alterations of cancer cells, and eclipsed the study of tumor bioenergetics, including Warburg's ideas.

Significance of the Warburg effect

The increasing number of recent reports on the Warburg effect has reestablished the significance of this effect in tumorigenesis, indicating that bioenergetics may play a critical role in malignant transformation. Furthermore, it has been reported that *TP53*, which is one of the most commonly mutated genes in cancer, can trigger the Warburg effect.[4] Glycolytic conversion is initiated in the early stages in cells that are genetically engineered to become cancerous, and the conversion was enhanced as the cells became more malignant.[5] Therefore, the Warburg effect might directly contribute to the initiation of cancer formation not only by enhanced glycolysis but also via decreased respiration in the presence of oxygen, which suppresses apoptosis.[6] This effect may also produce a metabolic shift to enhanced glycolysis and play a role in the early stages of multistep tumorigenesis *in vivo*.[7]

Embryonic stem (ES) cells and immortalized primary and cancerous cells show the common concerted metabolic shift, including enhanced glycolysis, decreased apoptosis, and reduced mitochondrial respiration; however, the mechanism underlying this shift is poorly characterized.[7] This finding reinforces the use of somatic stem cells or metastatic tumor cells in hypoxic niches. Hypoxia appears to regulate the functions of hematopoietic stem cells in the bone marrow[8] and metastatic tumor cells (M. Mori, unpublished data) by preserving important stem cell functions, such as cell cycle control, survival, metabolism, and protection against oxidative stress.

However, this idea is still a controversial topic;[3] one of the arguments suggest that the Warburg effect is the consequence of cancer, and not the main contributing factor of the disease. Nevertheless, several companies and laboratories, including ours, are now attempting to evaluate the bioenergetics associated with tumorigenesis by testing and challenging the available anticancer drugs.

The Warburg effect is now the basis for positron emission tomography (PET), a highly sensitive noninvasive technique used in pre-clinical and clinical imaging of cancer biology; this technique has facilitated early diagnosis and better management of oncology patients.[9] With greater acceptance, it should become an increasingly important technique for cancer imaging in the next decade.[9]

CANCER STEM CELL HYPOTHESIS

The hypothesis

In 1937, Furth and Kahn[10] showed that leukemia can be initiated in mice using a single tumorigenic cell. This gave rise to a notion that a single or a few malignant cells, which have been transformed from normal somatic cells, can produce tumors. During the turn of the 21st century, the CSC hypothesis has gained recognition again, mainly in the Western world. After the identification of rare CSCs in leukemia,[11-13] molecular markers for detecting CSCs in solid tumors, such as head and neck,[14] breast,[15] and brain cancers,[16,17] have also been identified. The research team at one of our laboratories has obtained the first evidence of CSCs in the gastrointestinal system,[18] and our findings have subsequently been confirmed by other researchers.[19,20]

Significance of the hypothesis

A small population of cancer-initiating cells plays a very important role, in that it may cause resistance to chemotherapy or radiation therapy or lead to post-therapy recurrence even when most of the cancer cells appear to be dead.[21] In addition to their genetic alterations, CSCs are believed to mimic normal adult stem cells with regard to properties like self renewal and undifferentiated status, which eventually leads to the formation of differentiated cells.[22] Moreover, unlike well-differentiated daughter cells, small populations of CSCs are believed to be more resistant to toxic injuries and chemoradiotherapy.[23] Whereas the conventional cancer therapies have always been targeted toward proliferating cells, the control of CSCs, which is often exercised in the dormant phase of the cell cycle, can now be applied to achieve complete tumor regression.

Identification of cancer-specific markers

Due to their potential use in clinical applications, the surface markers of CSCs have been studied and identified. Adult stem cells and their malignant counterparts share similar intrinsic and extrinsic factors that regulate the self renewal, differentiation, and proliferation pathways.[24] The following are the examples of candidate markers: musashi-1 (Msi-1),[25] hairy and enhancer of split homolog-1 (Hes-1),[26] CD133 (prominin-1, Prom1),[27,28] epithelial cellular adhesion molecule (EpCam),[29] claudin-7,[29] CD44 variant isoforms,[29] Lgr5,[30]

Hedgehog (Hh),[31] bone morphogenic protein (Bmp),[32,33] Notch,[34] and Wnt.[35] Nevertheless, little is known about the molecular markers that are characteristic of dormant stem cells and amplified populations of differentiating cells of solid tumors, such as the tumors of the gastrointestinal tract.[35]

BIOENERGETICS OF CANCER STEM CELLS

The bioenergetics associated with the adaptation of CSCs to their microenvironment still requires extensive research. Although numerous studied suggested the association between Warburg effect and reduced oxidative stress in cancer, the relevant molecular mechanism was not known until very recently when Ruckenstuhl, et al.[6] reported their findings in a yeast model.

Hypoxic adaptations in the presence of oxygen

Through different biochemical and biophysical pathways, which are characteristic to cancer cells, tumor cells adopt this phenotype, i.e., high glycolysis and decreased respiration, in the presence of oxygen. It has been shown that although the induction of hypoxia and cellular proliferation engage entirely different cellular pathways, they often coexist during tumor growth.[36] The ability of cells to grow during hypoxia results, in part, from the crosstalk between hypoxia-inducible factors (Hifs) and the proto-oncogene c-Myc.[36] These genes partially regulate the development of complex adaptations of tumor cells growing in low O_2, and contribute to fine tuning the adaptive responses of cells to hypoxic environments.[36] Nevertheless, how cancer cells achieve one of the most common phenotypes, namely, the "Warburg effect," i.e., elevated glycolysis in the presence of oxygen, is still a topic of hypothesis, unless the involvement of glycolysis genes is considered.

Recently, it was shown that the hexokinase 2 (Hk-2) protein, its mitochondrial receptor, namely, voltage-dependent anion channel (Vdac), and the gene encoding Hk-2 play the most pivotal and direct roles in the "Warburg effect," despite some impairment in the respiratory capacity of malignant tumors is involved.[37] Furthermore, metabolic reprogramming during physiologic cell proliferation and tumorigenesis may alter cell growth and proliferation by modifying the flux of cellular mediators of signal transduction and gene expression, including the expression of phosphatidylinositol 3-kinase (PI3K)/Akt/mTOR system, hypoxia-inducible factor 1 (Hif-1), and Myc.[38] In particular, the genes of many glycolysis enzymes are under the control of Myc, Hif-1, and tumor suppressor p53,[7] suggesting that enhanced glycolysis is essential for both immortalization and transformation, since it renders cells resistant to oxidative stress and adaptive to hypoxic condition.[7]

Low oxidant levels in the niche

A study on hematopoietic stem cells revealed that low levels of reactive oxygen species are present in the bone marrow.[39] A low-oxygen niche in the bone marrow limits reactive oxygen species production, thus providing hematopoietic stem cells with a long-term protection from reactive oxygen species stressors such as senescence, apoptosis, and DNA damage.[39] The research indicated that it is possible to isolate the early hematopoietic stem cell population by taking advantage of limited intracellular reactive oxygen species activity.[39] Thus, somatic stem cells such as those in the hematopoietic system reside in the hypoxic area in the bone marrow niche, which affords them protection from deleterious damages, presumably through the involvement of glycolytic metabolism.[39,40]

The Warburg effect has been observed in differentiating cancer cells (e.g., cells that undergo epithelial-to-mesenchymal and mesenchymal-to-amoeboid transition), cells resistant to anoikis, and cells which interact with the stromal components of the metastatic niche.[41] We showed that the epithelial-to-mesenchymal transition is involved in the resistance to chemotherapy in gastrointestinal cancer cells.[42] Cancer metastasis can be regarded as an integrated "escape program" triggered by redox changes.[41] These alterations might be associated with avoiding oxidative stress in the niche of the tumor cells, or presumably with the response to treatments aimed at genetic targets, such as chemotherapy and radiation. Regulation of reactive oxygen species in CSCs population is an important issue; we are investigating this topic by *in vitro* and *in vivo* experiments.

CONCLUSION

We studied the significance of bioenergetics of CSCs. Although the accomplishments of the genome project have contributed to cancer research and medicine, we have to pay more attention inimproving cancer diagnosis and therapy. In this article, we have highlighted the significance of a few relevant concepts, which have been recently discovered. Moreover, our study indicated that the introduction of induced pluripotent stem (iPS) cell genes was necessary for inducing the expression of immature status-related proteins in gastrointestinal cancer cells, and that the induced pluripotent cancer (iPC) cells were distinct from natural cancer cells with regard to their sensitivity to differentiation-inducing treatment.[43] For the complete eradication of cancer, however, future efforts should be directed toward improving translational research.

ACKNOWLEDGEMENTS

This work was supported in part by a grant-in-aid for scientific research from the Ministry of Education, Culture, Sports, Science, and Technology, Japan; and from Mitsubishi Pharma Research Foundation, Uehara Memorial Foundation, and Kobayashi Cancer Foundation, Japan.

REFERENCES

1. Nowell PC. Chromosomes and cancer: the evolution of an idea. Adv Cancer Res 1993;62:1-17.
2. Warburg O. On respiratory impairment in cancer cells. Science 1956;124:269-70.
3. Garber K. Energy deregulation: licensing tumors to grow. Science 2006;312:1158-9.
4. Matoba S, Kang JG, Patino WD, Wragg A, Boehm M, Gavrilova O, et al. p53 regulates mitochondrial respiration. Science 2006;312:1650-3.
5. Ramanathan A, Wang C, Schreiber SL. Perturbational profiling of a cell-line model of tumorigenesis by using metabolic measurements. Proc Natl Acad Sci U S A 2005;102:5992-7.
6. Ruckenstuhl C, Büttner S, Carmona-Gutierrez D, Eisenberg T, Kroemer G, Sigrist SJ, et al. The Warburg effect suppresses oxidative stress induced apoptosis in a yeast model for cancer. PLoS One 2009;4:e4592.
7. Kondoh H. Cellular life span and the Warburg effect. Exp Cell Res 2008;314:1923-8.
8. Eliasson P, Jönsson JI. The hematopoietic stem cell niche: low in oxygen but a nice place to be. J Cell Physiol 2010;222:17-22.
9. Gambhir SS. Molecular imaging of cancer with positron emission tomography. Nat Rev Cancer 2002;2:683-93.
10. Furth J, Kahn MC. The transmission of leukemia of mice with a single cells. Am J Cancer 1937;31:276-82.
11. Wulf GG, Wang RY, Kuehnle I, Weidner D, Marini F, Brenner MK, et al. A leukemic stem cell with intrinsic drug efflux capacity in acute myeloid leukemia. Blood 2001;98:1166-173.
12. Lapidot T, Sirard C, Vormoor J, Murdoch B, Hoang T, Caceres-Cortes J, et al. A cell initiating human acute myeloid leukaemia after transplantation into SCID mice. Nature 1994;367:645-8.
13. Bonnet D, Dick JE. Human acute leukemia is organized as a hierarchy that originates from a primitive hematopoietic cell. Nat Med 1997;3:730-7.
14. Prince ME, Sivanandan R, Kaczorowski A, Wolf GT, Kaplan MJ, Dalerba P, et al. Identification of a subpopulation of cells with cancer stem cell properties in head and neck squamous cell carcinoma. Proc Natl Acad Sci U S A 2007;104:973-8.
15. Al-Hajj M, Wicha MS, Benito-Hernandez A, Morrison SJ, Clarke MF. Prospective identification of tumorigenic breast cancer cells. Proc Natl Acad Sci U S A 2003;100:3983-8.
16. Piccirillo SG, Reynolds BA, Zanetti N, Lamorte G, Binda E, Broggi G, et al. Bone morphogenetic proteins inhibit the tumorigenic potential of human brain tumour-initiating cells. Nature 2006;444:761-5.
17. Bao S, Wu Q, McLendon RE, Hao Y, Shi Q, Hjelmeland AB, et al. Glioma stem cells promote radioresistance by preferential activation of the DNA damage response. Nature 2006;444:756-60.
18. Haraguchi N, Utsunomiya T, Inoue H, Tanaka F, Mimori K, Barnard GF, et al. Characterization of a side population of cancer cells from human gastrointestinal system. Stem Cells 2006;24:506-13.
19. Ricci-Vitiani L, Lombardi DG, Pilozzi E, Biffoni M, Todaro M, Peschle C, et al. Identification and expansion of human colon-cancer-initiating cells. Nature 2007;445:111-5.
20. O'Brien CA, Pollett A, Gallinger S, Dick JE. A human colon cancer cell capable of initiating tumour growth in immunodeficient mice. Nature 2007;445:106-10.
21. Tan BT, Park CY, Ailles LE, Weissman IL. The cancer stem cell hypothesis: a work in progress. Lab Invest 2006;86:1203-7.
22. Reya T, Morrison SJ, Clarke MF, Weissman IL. Stem cells, cancer, and cancer stem cells. Nature 2001;414:105-11.
23. Sagar J, Chaib B, Sales K, Winslet M, Seifalian A. Role of stem cells in cancer therapy and cancer stem cells: a review. Cancer Cell Int 2007;7:9.
24. Giordano A, Fucito A, Romano G, Marino IR. Carcinogenesis and environment: the cancer stem cell hypothesis and implications for the development of novel therapeutics and diagnostics. Front Biosci 2007;12:3475-82.
25. Nakamura M, Okano, H, Blendy JA, Montell C. Musashi, a neural RNA-binding protein required for Drosophila adult external sensory organ development. Neuron 1994;13:67-81.
26. Ishibashi M, Ang SL, Shiota K, Nakanishi S, Kageyama R, Guillemot F. Targeted disruption of mammalian hairy and Enhancer of split homolog-1 (HES-1) leads to up-regulation of neural helix-loop-helix factors, premature neurogenesis, and severe neural tube defects. Genes Dev 1995;9:3136-48.
27. Lin EH, Hassan M, Li Y, Zhao H, Nooka A, Sorenson E, et al. Elevated circulating endothelial progenitor marker CD133 messenger RNA levels predict colon cancer recurrence. Cancer 2007;110:534-42.
28. Mehra N, Penning M, Maas J, Beerepoot LV, van Daal N, van Gils CH, et al. Progenitor marker CD133 mRNA is elevated in peripheral blood of cancer patients with bone metastases. Clin Cancer Res 2006;12:4859-66.
29. Kuhn S, Koch M, Nübel T, Ladwein M, Antolovic D, Klingbeil P, et al. A complex of EpCAM, claudin-7, CD44 variant isoforms, and tetraspanins promotes colorectal cancer progression. Mol Cancer Res 2007;5:553-67.
30. Barker N, van Es JH, Kuipers J, Kujala P, van den Born M, Cozijnsen M, et al. Identification of stem cells in small intestine and colon by marker gene Lgr5. Nature 2007;449:1003-7.
31. Ingham PW, McMahon AP. Hedgehog signaling in animal development: paradigms and principles. Genes Dev 2001;15: 3059-87.
32. Koenig BB, Cook JS, Wolsing DH, Ting J, Tiesman JP, Correa PE, et al. Characterization and cloning of a receptor for BMP-2 and BMP-4 from NIH 3T3 cells. Mol Cell Biol 1994;14:5961-74.
33. ten Dijke P, Yamashita H, Sampath TK, Reddi AH, Estevez M, Riddle DL, et al. Identification of type I receptors for osteogenic protein-1 and bone morphogenetic protein-4. J Biol Chem 1994;269:16985-8.
34. Bray S. Notch signalling: a simple pathway becomes complex. Nat Rev Mol Cell Biol 2006;7:678-89.
35. Yen TH, Wright NA. The gastrointestinal tract stem cell niche. Stem Cell Rev 2006;2:203-12.
36. Gordan JD, Thompson CB, Simon MC. HIF and c-Myc: sibling rivals for control of cancer cell metabolism and proliferation.

Cancer Cell 2007;12:108-13.
37. Pedersen PL. Warburg, me and Hexokinase 2: Multiple discoveries of key molecular events underlying one of cancers' most common phenotypes, the "Warburg Effect", i.e., elevated glycolysis in the presence of oxygen. J Bioenerg Biomembr 2007;39: 211-22.
38. DeBerardinis RJ, Lum JJ, Hatzivassiliou G, Thompson CB. The biology of cancer: metabolic reprogramming fuels cell growth and proliferation. Cell Metab 2008;7:11-20.
39. Jang YY, Sharkis SJ. A low level of reactive oxygen species selects for primitive hematopoietic stem cells that may reside in the low-oxygenic niche. Blood 2007;110:3056-63.
40. Hosokawa K, Arai F, Yoshihara H, Nakamura Y, Gomei Y, Iwasaki H, et al. Function of oxidative stress in the regulation of hematopoietic stem cell-niche interaction. Biochem Biophys Res Commun 2007;363:578-83.
41. Pani G, Giannoni E, Galeotti T, Chiarugi P. Redox-based escape mechanism from death: the cancer lesson. Antioxid Redox Signal 2009;11:2791-806.
42. Hoshino H, Miyoshi N, Nagai K, Tomimaru Y, Nagano H, Sekimoto M, et al. Epithelial-mesenchymal transition with expression of SNAI1-induced chemoresistance in colorectal cancer. Biochem Biophys Res Commun 2009;390:1061-5.
43. Miyoshi N, Ishii H, Nagai Ki, Hoshino H, Mimori K, Tanaka F, et al. Defined factors induce reprogramming of gastrointestinal cancer cells. Proc Natl Acad Sci U S A 2010;107:40-5.

CD13 is a therapeutic target in human liver cancer stem cells

Naotsugu Haraguchi,[1,2] Hideshi Ishii,[1,3] Koshi Mimori,[3] Fumiaki Tanaka,[3] Masahisa Ohkuma,[4] Ho Min Kim,[1] Hirofumi Akita,[1] Daisuke Takiuchi,[1] Hisanori Hatano,[1] Hiroaki Nagano,[1] Graham F. Barnard,[5] Yuichiro Doki,[1] and Masaki Mori[1]

[1]Department of Gastroenterological Surgery, Graduate School of Medicine, Osaka University, Osaka, Japan. [2]Excellent Young Researchers Overseas Visit Program, Japan Society for the Promotion of Science (JSPS), Tokyo, Japan. [3]Department of Surgery, Medical Institute of Bioregulation, Kyushu University, Oita, Japan. [4]Department of Surgery, Jikei University School of Medicine, Tokyo, Japan. [5]Department of Medicine, University of Massachusetts Medical School, Worcester, Massachusetts, USA.

Cancer stem cells (CSCs) are generally dormant or slowly cycling tumor cells that have the ability to reconstitute tumors. They are thought to be involved in tumor resistance to chemo/radiation therapy and tumor relapse and progression. However, neither their existence nor their identity within many cancers has been well defined. Here, we have demonstrated that CD13 is a marker for semiquiescent CSCs in human liver cancer cell lines and clinical samples and that targeting these cells might provide a way to treat this disease. $CD13^+$ cells predominated in the G_0 phase of the cell cycle and typically formed cellular clusters in cancer foci. Following treatment, these cells survived and were enriched along the fibrous capsule where liver cancers usually relapse. Mechanistically, CD13 reduced ROS-induced DNA damage after genotoxic chemo/radiation stress and protected cells from apoptosis. In mouse xenograft models, combination of a CD13 inhibitor and the genotoxic chemotherapeutic fluorouracil (5-FU) drastically reduced tumor volume compared with either agent alone. 5-FU inhibited $CD90^+$ proliferating CSCs, some of which produce $CD13^+$ semiquiescent CSCs, while CD13 inhibition suppressed the self-renewing and tumor-initiating ability of dormant CSCs. Therefore, combining a CD13 inhibitor with a ROS-inducing chemo/radiation therapy may improve the treatment of liver cancer.

Introduction

Functional and morphologic heterogeneity exists in a tumor with a hierarchy in which tumor growth is driven by a small subset of cancer stem cells (CSCs) (1). Like normal tissue stem cells, which are capable of self renewal and multidifferentiation, CSCs have the ability to reconstitute tumors (2). In the hematologic cell lineage, stem cells exist in the dormant phase and can be detected as a side population (SP) (3). Generally, CSCs, like somatic tissue stem cells, proliferate slowly, i.e., they are in the dormant or slow-growing phase of the cell cycle. This partially accounts for their therapeutic refractoriness to chemo/radiation therapy, tumor relapse, and presumably metastasis. The CSCs of acute myeloid leukemia (4) and chronic myeloid leukemia (5) also survive in the dormant G_0 phase of the cell cycle in a bone marrow niche after chemotherapy. Relapses and metastases of breast cancer often occur after intervals of several decades, suggesting the involvement of a deep dormant phase for CSCs (6). The majority of liver cancers are superimposed on a background of chronic hepatitis and hepatic cirrhosis. Therefore, it may be difficult to distinguish between intrahepatic metastasis through portal or hepatic venules and metachronous multicentric development of liver cancer in a precancerous background. However, there are some cases of liver cancer in which cancer recurs in the liver or metastasizes to the lung and bone several years after radical hepatectomy or liver transplantation. This suggests that some slow-growing cancer cells also exist in liver cancer but these may not be in deep dormancy like breast cancer CSCs.

Anticancer reagents in clinical use generally affect division and proliferation of cancer cells. This could result in elimination of proliferating cancer cells but not reduce the survival of CSCs in the dormant or slow-growing phase. Thus, the identification and characterization of dormant or slow-growing CSCs are important for developing novel therapeutic approaches.

In studies of hepatocellular carcinoma (HCC) (7), the fifth most common cancer in the world, the SP fraction (8), $CD133^+$ (9–11), $CD44^+$ (11, 12), $CD90^+$ (12, 13), and epithelial cell adhesion molecules (14) were reported as markers of CSCs or cancer-/tumor-initiating cells. The majority of CSC studies focus on identification of cell markers to enrich cell populations that have high tumor initiation ability in immune-deficient mice. In the field of liver cancer CSCs, there have been few reports describing dormant or slow-growing CSCs that include their cellular characteristics or indicate a way to target these cells based on cytological evidence. In addition, there have been few reports that clearly indicate the interrelationships among these candidate markers.

In a previous study (similar to hematopoietic and leukemic studies), we reported that the SP fraction enriches the CSC-like fractions. Cells of the SP fraction express both hepatocyte and cholangiocyte markers, show high resistance to anti-cancer agents, and high tumorigenicity in NOD/SCID mice (8). Based on our previous data (8) and applying the techniques of hematopoietic stem cell studies (3–5), our aims were as follows: first, to clarify the relationships between reported candidate CSC markers; second, to assess whether dormant CSCs exist in liver cancer and to concentrate on cell-surface markers, which definitively identify potentially dormant CSCs; third, to clarify the cellular characteristics of potentially dormant CSCs and to identify the mechanisms that protect potentially dormant CSCs from chemo/radiation therapy; finally, to identify target molecules of liver cancer CSCs to initiate novel approaches that could lead to a future radical cure for liver cancer.

Conflict of interest: The authors have declared that no conflict of interest exists.
Citation for this article: *J Clin Invest.* 2010;120(9):3326–3339. doi:10.1172/JCI42550.

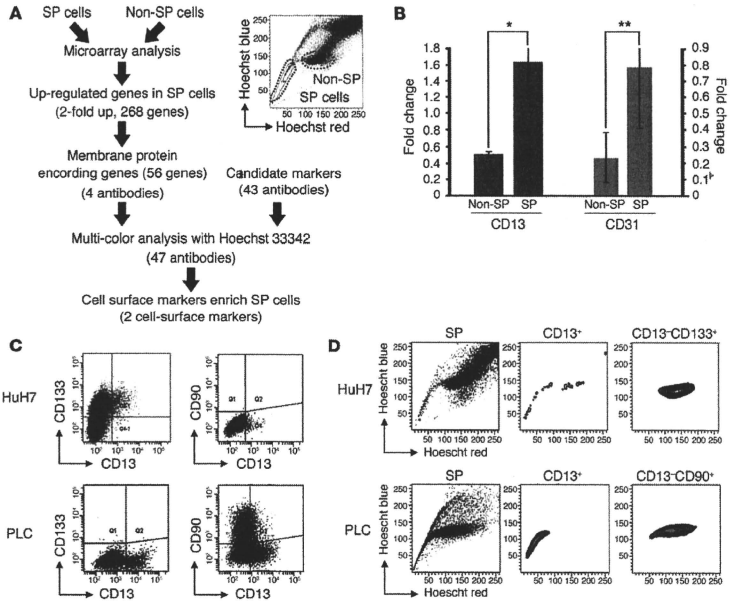

Figure 1

CD13 is a candidate marker of the SP fraction. (**A**) The strategy used to identify cell-surface markers closely related to the SP fraction. We determined CD13 and CD31 as candidate markers for identifying SP cells. (**B**) Both CD13 and CD31 expression in HuH7 cells were compared in SP and non-SP cells by semiquantitative RT-PCR. Data represent mean ± SD from independent experiments of fractions differentially sorted by flow cytometry. $^*P < 0.01$; $^{**}P = 0.076$ versus non-SP fractions. The cut-off lines were determined using isotype controls. (**C**) Expression of CD13, CD133, and CD90 in HuH7 (upper panels) and PLC/PRF/5 cells (lower panels). Horizontal and vertical axes denote expression intensity. (**D**) The SP fraction is recognized as a "beak" appearing beside the G_1 phase fraction. The relationship between $CD13^+$ and $CD13^-$ cells and the SP fraction was studied using multicolor flow cytometry.

Results

CD13 is a candidate marker closely correlated with SP cells. To identify specific cell-surface markers that correlate with the SP fraction, we utilized our previous data sets of SP and non-SP fraction gene expression profiles obtained using microarray analyses (8). From a list of 268 genes upregulated in the SP cells (with a fold change > 2) (8), we selected 56 genes that potentially encode cell-surface proteins via the UniProtKB database (http://www.uniprot.org/). Working from the list of 56 upregulated genes (Supplemental Table 1; supplemental material available online with this article; doi:10.1172/JCI42550DS1) and an additional 43 markers reported to be closely associated with normal stem cells and CSCs, we tested 47 commercially available antibodies (Supplemental Table 2) to identify surface markers that were enriched in the SP fraction (Figure 1A).

During this screening, we identified 2 candidate markers, CD13 and CD31. The expression analysis of CD13 was 1.64 ± 0.45 in the SP and 0.51 ± 0.03 in the non-SP cell fraction ($P < 0.01$) (Figure 1B). We focused on CD13 in the current study, since the expression of CD31 was abundant in the G_2/M/SP fraction but was not universal in the liver cancer cell lines studied by us (HuH7, PLC/PRF/5, and Hep3B), and the statistical significance was weak ($P = 0.076$) (Figure 1B and Supplemental Figure 1, A and B).

Expression of CD13, CD133, and CD90 was assessed in hepatitis infection–negative (HuH7) and –positive (PLC/PRF/5) cell lines. The expression of CD133 was detected in HuH7 but not in PLC/PRF/5, and the expression of CD90 was detected in PLC/PRF/5 but not in HuH7. The expression of CD13 was observed in both these cell lines as well as in Hep3B (Figure 1C and Supplemental Figure 1A). In HuH7 in particular, the $CD13^+$ cells typically existed in a $CD133^{strong}$ fraction ($CD13^+CD133^+$).

Multicolor analysis with Hoechst staining exhibited clear localization of $CD13^+$ cells in the SP fraction of HuH7 and PLC/PRF/5, whereas the $CD13^-CD133^+$ and $CD90^+$ fractions were localized to the G_1-to-G_2 fraction and not the SP fraction (Figure 1D). To confirm the cell-cycle status of the $CD13^+$ cells in PLC/PRF/5, cell-cycle analysis by combined multicolor analysis and 7-amino-actinomy-

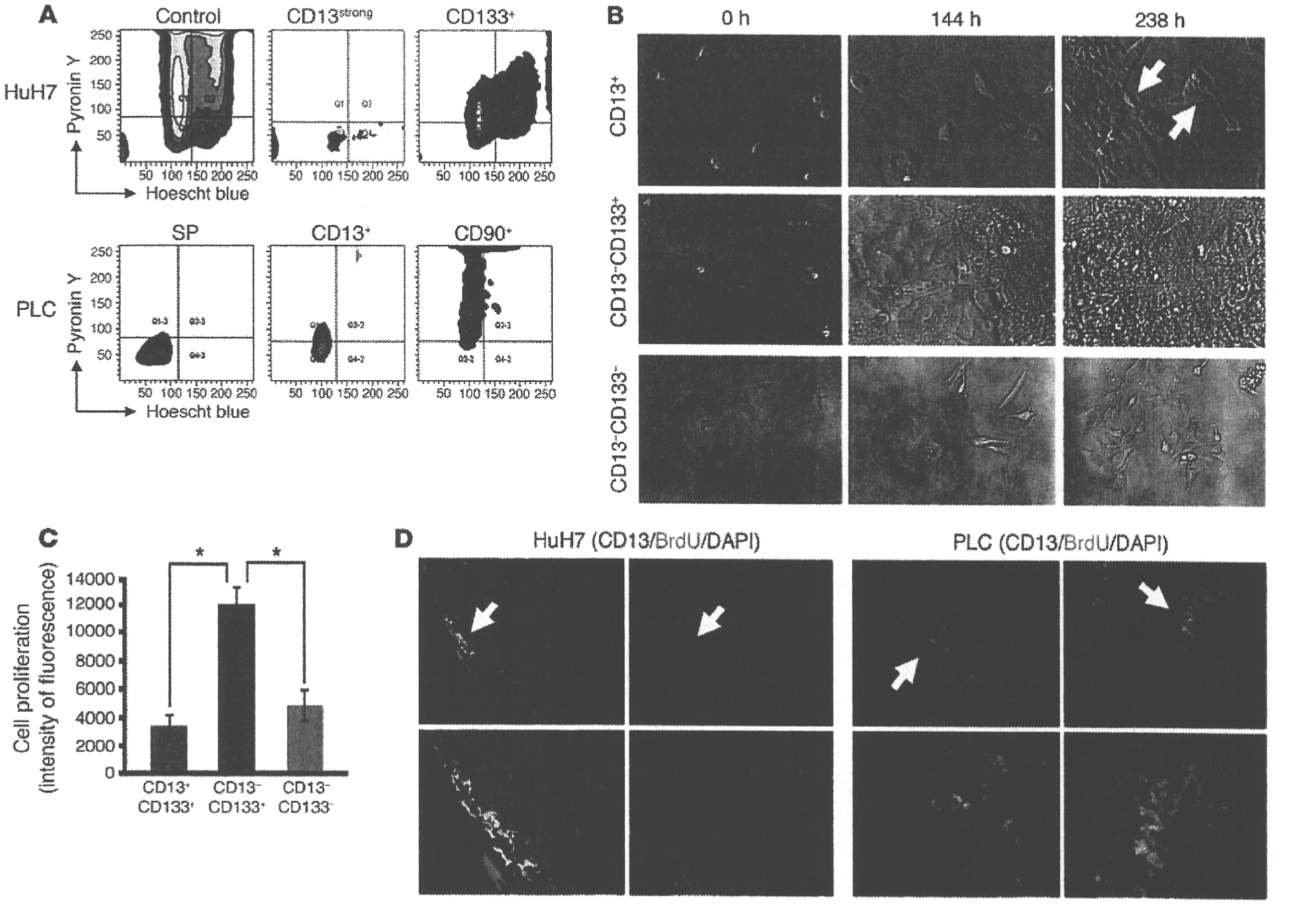

Figure 2

CD13 is a candidate marker of dormant to slow-growing CSCs. (**A**) Dormant cells can be identified using the DNA-binding dye Hoechst 33342 and RNA-binding dye PY. Dormant cells contain lower RNA levels than G_1 phase cells. Combination analysis of the cell cycle with cell-surface markers CD13, CD133, and CD90 was performed with reserpine. The cut-off lines were determined using isotype controls. (**B**) Time-lapse cell-fate tracing of HuH7 cells. Cells were labeled with PKH26GL, isolated to their $CD13^+$, $CD13^-CD133^+$, and $CD13^-CD133^-$ fractions, and traced for 238 hours. The dye-retaining cells can be identified as red-labeled cells (white arrow). Original magnification, ×20. (**C**) Proliferation assay of the $CD13^+CD133^+$, $CD13^-CD133^+$, and $CD13^-CD133^-$ fractions. Data represent mean ± SD from independent experiments of fractions differentially sorted by flow cytometry. $^*P < 0.05$. (**D**) BrdU-retaining cells in serially transplanted control tumor specimens of HuH7 (6 weeks after BrdU injection) and PLC/PRF/5 (10 weeks after BrdU injection). The sections were stained with anti-CD13 (red), BrdU (green), and DAPI (blue). Top panels show lower magnification of the sections of HuH7 and PLC/PRF/5 (×10, HuH7 and left panel of PLC; ×20, right panel of PLC). The lower panels show high magnification (×40) of the place indicated by white arrows in the top panels.

cin D (7-AAD) DNA labeling was performed. The $CD13^+CD90^-$ population was mainly in the G_0/G_1 phase, and the $CD13^+CD90^+$ population was clearly in the S to G_2/M phase. The $CD13^-CD90^+$ cells were present in all phases of the cell cycle but were more clearly present in the G_2/M and S phases when compared with the $CD13^+CD90^-$ population (Supplemental Figure 1C).

In these studies, we confirmed CD13 as a universal candidate marker that correlates with the liver cancer SP fraction. There were no definitive single markers that showed a stronger correlation to the SP fraction than CD13 and, to a lesser extent, CD31.

CD13 is a marker of tumor-initiating and potentially dormant HCC cells. Given that hematopoietic and leukemic stem cells are in the G_0 phase, identification and characterization of dormant or slow-growing cancer cell populations is very important because of these populations' relevance to chemo resistance and recurrence. Studies of CD13 expression in HuH7 and PLC/PRF/5 and their relationships with the cell-cycle phase, using the DNA-binding dye Hoechst 33342 and the RNA-binding dye pyronin Y (PY) (3), indicated that most of the $CD13^+$ fraction exists in the G_1/G_0 phase and the $CD13^{strong}$ population was clearly localized in G_0. The $CD133^+$ population in HuH7 and the $CD90^+$ fraction in PLC/PRF/5 were distributed in the G_1/G_0 and G_2/M phases, respectively. The relationships between the SP fraction and the G_0 cell-cycle phase were also confirmed, and the SP fraction was clearly localized in the G_0 phase under reserpine-free (ABC transporter blocker) conditions (Figure 2A).

To study the cell fate and dye-retaining capacity of HuH7 $CD13^+$ cells, the cell-surface membrane was labeled with PKH26GL reagent and cell fate was traced for 238 hours. Equal numbers of cells were seeded for each population. The $CD13^+CD133^+$ fraction exhibited very slow growth compared with the $CD13^-CD133^+$ fraction, with the doubling time of the $CD13^+CD133^+$ fraction estimated

Table 1
Limiting dilution and serial transplantation assay of HuH7 and PLC/PRF/5 cells

Cell type	Assay	Marker/cells	1×10^2	5×10^2	1×10^3	5×10^3	1×10^4
HuH7	Limiting dilution	$CD13^+CD133^+$	2/4	2/4	3/4	3/4	–
HuH7	Limiting dilution	$CD13^-CD133^+$	0/4	0/4	3/4	4/4	–
HuH7	Limiting dilution	$CD13^-CD133^-$	0/4	0/4	0/4	0/4	–
HuH7	Serial transplantation	$CD13^+CD133^+$	0/4	1/4	3/4	4/4	3/4
HuH7	Serial transplantation	$CD13^-CD133^+$	0/4	0/4	0/4	0/4	1/4
HuH7	Serial transplantation	Control	0/4	0/6	0/6	0/6	2/6
PLC	Limiting dilution	$CD13^+CD90^-$	2/4	2/2	4/4	3/3	–
PLC	Limiting dilution	$CD13^-CD90^+$	0/4	2/2	4/4	3/3	–
PLC	Limiting dilution	$CD13^-CD90^-$	0/4	0/4	0/3	0/4	–
PLC	Serial transplantation	$CD13^+CD90^-$	0/4	2/4	3/4	3/4	3/4
PLC	Serial transplantation	$CD13^-CD90^+$	0/4	0/4	0/4	0/4	1/4
PLC	Serial transplantation	Control	0/6	0/6	0/6	1/6	2/6

at approximately 160 hours. Dye-retaining cells could be observed 238 hours after cell seeding only in the $CD13^+CD133^+$ fraction (Figure 2B and Supplemental Videos 1–3). The $CD13^-CD133^-$ fraction exhibited cell fragmentation and apoptotic changes during cell culture. To confirm CD13 expression in association with cell growth, we performed cell proliferation assays. Data from isolated HuH7 populations showed that $CD13^+CD133^+$ cells exhibited slow cell growth compared with $CD13^-CD133^+$ cells 72 hours after seeding (Figure 2C). The $CD13^-CD133^-$ population also grew slowly but maintained viability for a week, with difficulty, because of apoptosis.

Next, tumor-formation ability of each fraction was studied in HuH7 and PLC/PRF/5 cells. Limiting dilution analysis of HuH7 cells revealed that the $CD13^+CD133^+$ fraction formed tumors from 100 cells (2/4), the $CD13^-CD133^+$ fraction formed tumors from 1,000 cells (3/4), and the $CD13^-CD133^-$ fraction formed no tumors from 5,000 cells (0/4) in NOD/SCID mice after 4 weeks of observation. In PLC/PRF/5 cells, the $CD13^+CD90^-$ fraction formed tumors from 100 cells (2/4), and the $CD13^-CD90^+$ fraction formed tumors from 5,000 cells (2/2), whereas the $CD13^-CD90^-$ cells formed no tumors from 5,000 cells (0/4) in NOD/SCID mice after 6 weeks of observation (Table 1). To assess the tumor formation ability definitively, formed tumors were digested, and isolated $CD13^+CD133^+$ and $CD13^-CD133^+$ fractions of HuH7 and isolated $CD13^+CD90^-$ and $CD13^-CD90^+$ fractions of PLC/PRF/5 were serially transplanted to secondary NOD/SCID mice. As controls, non-isolated cell fractions of HuH7 and PLC/PRF/5 were also serially transplanted. Tumor formation ability of $CD13^+$ cells compared with that of $CD13^-$ cells in serial transplantation assay was demonstrated more clearly than that of limiting dilution assay. In HuH7, after 6 weeks of observation, the $CD13^+CD133^+$ fraction formed tumors from 500 cells (1/4), whereas the $CD13^-CD133^+$ fraction and control formed very small tumors only in 10,000 cells (1/4 in the $CD13^-CD133^+$ fraction, and 2/6 in control). In PLC/PRF/5, after 6 weeks of observation, the $CD13^+CD90^-$ formed tumors from 500 cells (2/4), and the control formed tumors from 5,000 cells (1/6), whereas the $CD13^-CD90^+$ fraction formed 1 very small tumor only in 10,000 cells (1/4) (Table 1).

To assess semiquiescent status of $CD13^+$ cells in vivo, BrdU-retaining status was studied. Tumors obtained from NOD/SCID mice xenografted with HuH7 and PLC/PRF/5 cells were digested to single cells and serially transplanted without isolation of cell-surface markers. BrdU was injected intraperitoneally. After 6 weeks for HuH7, and after 10 weeks for PLC/PRF/5, tumors were enucleated and sections were stained with anti-BrdU and anti-CD13 antibody. In the tumors derived from HuH7 cells, very small numbers of BrdU-retaining cells that also expressed CD13 were observed typically in the edge of tumor foci. BrdU-retaining cells were not observed in the tumor center. Tumors derived from PLC/PRF/5 cells grew more slowly than did those derived from HuH7 cells. BrdU-retaining cells could be identified and did express CD13. Interestingly, clusters of $CD13^+BrdU^-$ cells were observed close to $CD13^+BrdU^+$ cells, suggesting that they might be derived from the $CD13^+BrdU^+$ cells (Figure 2D).

HCC-$CD13^+$ cells form spheres and produce the $CD90^+$ phenotype. Sphere formation is a common characteristic of stem cells. To evaluate CD13 as a candidate CSC marker, the expression of CD13 in spheres derived from HuH7, PLC/PRF/5, and clinical HCC was studied. The expression of CD13 was increased in both HuH7 (2.0% in control vs. 67.0% in spheres; 33.5-fold increase) and PLC/PRF/5 (15.2% in control vs. 83.8% in spheres; 5.51-fold increase) (Figure 3A). There was no significant change in CD133 expression in HuH7. In PLC/PRF/5, expression of CD90 was decreased in the spheres (35.7% in control vs. 2.5% in spheres; 14.28-fold decrease). The expression of CD13 compared with that of CD133 and CD90 appeared to be associated with a more immature stem-like and dormant population. Spheres established from clinical HCC samples localized in the $CD13^+CD90^-CD133^-$ fraction in a manner similar to that observed in PLC/PRF/5 (Figure 3B).

The time-course changes in the expression of CD13 and CD90 in PLC/PRF/5 were studied. Isolation and culture of the $CD13^+CD90^-$ fraction from the PLC/PRF/5 spheres in serum-containing media resulted in the production of $CD13^+CD90^+$ fraction after 96 hours (Figure 3C). The isolated $CD13^-CD90^-$ fraction elicited cell death within a few days and could not be maintained. Interestingly, the isolated $CD13^-CD90^+$ fraction rapidly produced the $CD13^+CD90^-$ fraction within 24 hours (Figure 3C). These findings suggest that potentially dormant $CD13^+$ cells produce proliferating $CD90^+$ cells and that some parts of the proliferating $CD90^+$ cells also produce $CD13^+$ cells. It is important to determine how this $CD13^+$ population (slow-growing potentially dormant) could be maintained in a cancer cell line in vitro. Dormant or slow-growing cell populations may disappear during continuous subculturing. These findings may replicate the rapid change from dormant to active status in cancer stem-like cells, as revealed by their cell-surface markers, or the dormant cells might mimic a certain multipotent condition in cellular differentiation.

$CD13^+$ cells resist chemotherapy, and CD13 inhibition drives cells to apoptosis. The change of cell-surface marker expression before and after doxorubicin (DXR) hydrochloride treatment or 5-fluorouracil (5-FU) was studied in HuH7 and PLC/PRF/5. In HuH7, CD13

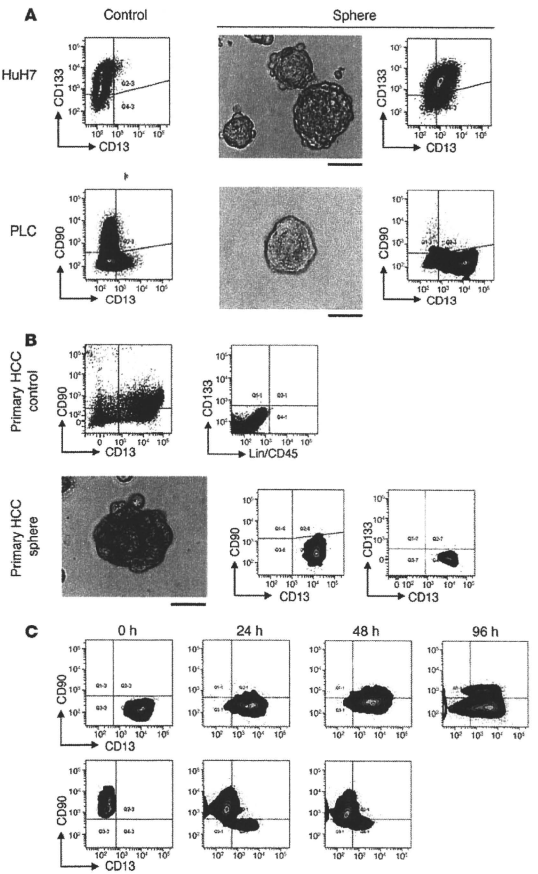

Figure 3

CD13⁺ cells exist as a core in HCC spheres and produce CD90⁺ cells. (**A**) Spheres established from HuH7 and PLC/PRF/5 cells were dissociated to single cells and the marker expressions were compared with control cells. Scale bars: 200 μm. (**B**) Expression analysis of primary human HCC cells (control) and spheres established from original human HCC cells (sphere). Scale bar: 200 μm. (**C**) The time-course expression analyses of sorted CD13⁺CD90⁻ cells (upper panels) and CD13⁻CD90⁺ cells (lower panels) from PLC/PRF/5. The cut-off lines were determined using isotype controls.

expression was increased over 20-fold by DXR or 5-FU treatment compared with control ($CD13^+CD133^+$ population in control, 2.0%; by DXR treatment, 40.3%; by 5-FU treatment, 44.3%), although expression of CD133 remained unchanged (87.1% in control vs. 88.0% after DXR treatment, 88.7% after 5-FU treatment). In PLC/PRF/5, after treatment with DXR, the $CD13^+CD90^-$ fraction was also increased and the $CD13^-CD90^+$ fraction was shifted to the CD13 positive (the $CD13^+CD90^-$ fraction of control was 15.4% and of DXR treatment was 58.2%). After treatment with 5-FU, the remaining cells were more clearly localized in the $CD13^+CD90^-$ fraction (77.8%) (Figure 4A). The chemo-resistance ability of the $CD13^+$ cells was also confirmed by cell proliferation assay in HuH7. The $CD13^+CD133^+$ fraction was highly resistant to DXR compared with the $CD13^-CD133^+$ and $CD13^-CD133^-$ fractions, indicating consistent changes in the markers following DXR treatment (Supplemental Figure 2A). Although the $CD13^-CD133^-$ fraction exhibited slow cell growth in the proliferation and cell fate study (Figure 2, B and C), this fraction showed high chemosensitivity.

Next, the effect of CD13 inhibition on cell proliferation in HuH7 was assessed. Cell proliferation was suppressed in a concentration-dependent manner after 72 hours exposure to the CD13-neutralizing antibody. At 10 and 20 μg/ml concentrations of the CD13-neutralizing antibody, cell proliferation was suppressed by approximately 80% at 24 hours and 95% at 72 hours (Figure 4B). The apoptosis assay showed that both the CD13-neutralizing antibody and CD13 inhibitor ubenimex induced apoptosis in both HuH7 and PLC/PRF/5 after 24 hours (Figure 4C). The CD13 antibody (clone WM15) has been shown to be specific to humans and to function as a neutralizing antibody (15). Reportedly, ubenimex (bestatin) specifically blocks CD13, which antagonizes the zinc-binding site of the aminopeptidase N domain (16–19). Ubenimex is used as a therapeutic agent for adult acute nonlymphatic leukemia (20).

We then hypothesized that not only the ABC transporter (21, 22) but also CD13 is involved in cell protection against exposure to anticancer agents. DXR is a well-known ABC-transporter–dependent anticancer drug. We have established a DXR-resistant HuH7 clone in which 90% of cells survive in 0.5 μg/ml of DXR, whereas about 99% of parent HuH7 cells die at that concentration (Supplemental Figure 2, B and C). Inhibition of CD13 indicated approximately 50% suppression of cell proliferation in this clone (Figure 4D), and this finding suggests that CD13 inhibition can potentially suppress cells that may have multidrug-resistance capacities and remain viable after conventional anticancer drug treatments.

CD13 is expressed preferentially in therapy-resistant HCC cells. To identify the expression of CD13 in clinical HCC, HCC samples were digested and hematopoietic Lin^-CD45^- fractions were further

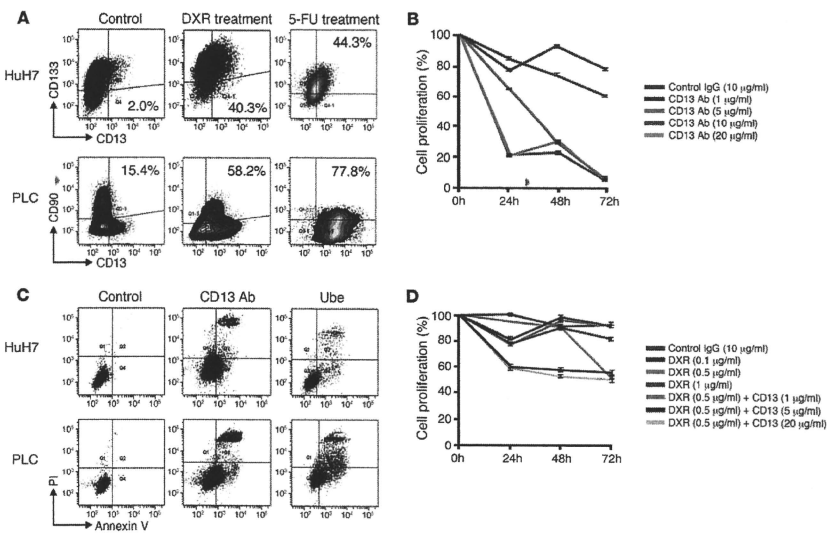

Figure 4

CD13⁺ cells resist chemotherapy, and inhibition of CD13 elicits cellular apoptosis. (**A**) The HuH7 and PLC/PRF/5 cells were treated with 0.1 μg/ml of DXR or 1 μg/ml of 5-FU for 72 hours. The changes in cell-surface markers were compared with controls. The percentages of $CD13^+CD133^+$ in HuH7 and $CD13^+CD90^-$ populations in PLC/PRF/5 are shown in figure. (**B**) Effect of CD13 inhibition on cell proliferation. HuH7 cells were treated with various concentrations of anti-human mouse IgG_1 CD13-neutralizing antibody. As a negative control, 10 μg/ml of anti-human mouse IgG_1 antibody was used. (**C**) Inhibition of CD13 induces cell apoptosis. Cells were treated with 1–20 μg/ml of CD13-neutralizing antibody or 50–500 μg/ml of ubenimex for 24 hours. Data show each case of 5 μg/ml of CD13-neutralizing antibody and 100 μg/ml of ubenimex treatment. (**D**) The effect of CD13-neutralizing antibody on DXR-R HuH7. The DXR-R clone was established with continuous treatment in 1 μg/ml of DXR and a selection of viable colonies. In 0.5 μg/ml of DXR, most control HuH7 cells die after 72 hours, whereas over 90% of DXR-R cells survive. The DXR-R HuH7 cells were cultured with 1–20 μg/ml of CD13-neutralizing antibody for 72 hours. Control, treated with 10 μg/ml of anti-human mouse IgG_1 antibody.

analyzed by multicolor flow cytometry. In all 12 clinical HCC samples, including 3 cases of non-hepatitis-derived HCC (1 case recurred after transcatheter arterial embolization [TAE]) and 9 cases of hepatitis-derived HCC (4 cases recurred after TAE), no CD133 expression was observed. In all cases, CD13 and CD90 expression was observed in the following 4 subpopulations: $CD13^+CD90^+$, $CD13^+CD90^-$, $CD13^-CD90^+$, and $CD13^-CD90^-$. In cases that recurred after TAE, the $CD13^+CD90^-$ fraction was more abundant than that in non-TAE cases (48% ± 12% in TAE cases vs. 8% ± 4% in non-TAE cases; 6-fold increase), whereas the $CD13^-CD90^+$ fraction was more abundant in non-TAE cases than in TAE cases (40% ± 18% in non-TAE cases vs. 12% ± 5% in TAE cases; 3.3-fold increase) (Figure 5A). In all 12 clinical HCC samples, the expression patterns were very similar to that of PLC/RLF/5, indicating its usefulness as an HCC model. Of course, the percentages of cells just indicate the percentage that survived after mechanical and enzymatic digestion. The majorities of HCC cells retain the cellular functions of liver cells, accumulate fat and glycogen, and produce bilirubin. Also, they are relatively bigger than other kinds of cancer cells and may be more easily damaged by mechanical and enzymatic digestion.

The expression of CD13 was confirmed in fresh frozen surgical specimens. The $CD13^+$ HCC cells typically existed along the fibrous capsule forming cellular clusters after TAE. In non-TAE cases, the $CD13^+$ HCC cells usually formed small cellular clusters inside the cancer foci (Figure 5B). CD13 was expressed on the cell surface in HCC cases. In normal liver samples, CD13 was expressed in the sinusoid with a linear staining pattern and in bile ducts with an intraductal pattern; this was different in the HCC samples. The immunohistochemical findings for the post-TAE cases support clinical experience because HCC recurrence after TAE usually occurs at the fibrous capsule and chemoresistant viable HCC cells exist mainly around the fibrous capsule.

Interestingly, some small canalicular structures near the bile ducts expressed CD13 on the cell surface, and these are suggested to be liver stem/progenitor cells, since it has been reported that normal liver stem/progenitor cells express CD13 (23). In our studies, spheres established from the normal liver were predominantly

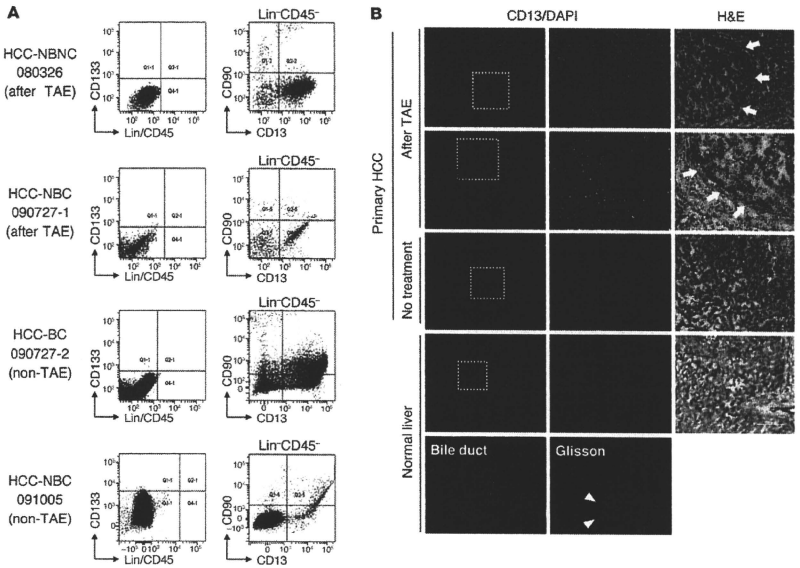

Figure 5

CD13 expression in clinical HCC samples with or without TAE. (**A**) Expression analysis of clinical HCC samples. The nonhematopoietic Lin/CD45$^-$ fraction was analyzed. The data show 2 typical TAE and non-TAE cases, nonhepatitis virus infection (NBNC; first row), nonhepatitis B but hepatitis C infection (NBC; second row), both hepatitis B and C infection (BC; third row), and another nonhepatitis B but hepatitis C infection (fourth row). The cut-off lines were determined using isotype controls. (**B**) Immunohistochemical analysis of HCC and normal liver samples stained with anti-human CD13 (red) and DAPI (blue) for the nucleus. Each middle panel shows a high magnification (×40) of the white dotted square in each left-hand column (×10). The right columns exhibit H&E stains (×10) of each adjacent frozen section. 3 typical samples from 6 HCC samples are represented. The white arrow indicates the fibrous capsule (Fc) in HCC samples, and tumor cells exist inside Fc. The upper 2 samples show HCC after TAE, and the middle samples are from no-TAE cases. In HCC samples, CD13 is expressed on the cell surface. The lower panels show immunohistochemical stains of normal liver obtained from surgical sections of colon cancer metastasis. Expression of CD13 in hepatic lobules is linear along the sinusoid. In the bile ducts, CD13 is expressed in an intraductal manner (lower left; bile duct, ×40). In some small canalicula present near the bile duct, CD13 is expressed on the cell surface (lower right; Glisson, ×40).

CD13$^+$CD90$^+$CD133$^+$, with a multidifferentiation potential in both hepatocyte and cholangiocyte lineages (Supplemental Figure 3).

To assess whether the area of the fibrous capsule contributed to the maintenance of semiquiescent CD13$^+$ cells, we stained fresh frozen tissues obtained from HCC parents with a hypoxia marker, carbonic anhydrase 9 (CA9) (24). In hematopoietic stem cells, hypoxia is well known as a hypoxic niche that plays important roles in maintaining stem cells in a dormant phase (25, 26). In the TAE samples, expression of CA9 was localized along the fibrous capsule and coexpressed CD13. In the non-TAE samples, CA9$^+$ cells formed cellular clusters in cancer foci and coexpressed CD13. In normal livers, CA9 expression was limited to the cell surface of bile ducts (Supplemental Figure 4).

CD13 inhibition elicits tumor regression. For preliminary studies, HuH7 cells were transplanted into NOD/SCID mice and treated with 5-FU to determine whether the CD13$^+$ fraction was enriched by treatment with a DNA synthesis inhibitor or not. We used 5-FU, the most common anticancer drug in HCC treatment, to simulate the clinical setting. After 3 days of intraperitoneal administration of 5-FU (30 mg/kg), most Ki67$^+$ active cells were disrupted and remained only at small foci, and tumors were replaced by a majority of CD13$^+$Ki67$^-$ cells. In the controls, CD13 expression was limited to a small fraction with cellular clustering, and most cells expressing CD13 were Ki67$^-$. Conversely, in ubenimex-treated mice (20 mg/kg, 3 days), most of the CD13$^+$ cells were disrupted and replaced with Ki67$^+$ active cells (Figure 6A).

PLC/PRF/5 was then used for further analyses. The expression of markers in this cell line is similar to that in clinical HCC, and thus, the PLC/PRF/5 cell line is potentially useful as an HCC model. In control mice, CD13 expression was limited to a small fraction and most of the cells expressed CD90. After treatment with 5-FU (30 mg/kg, 5 days of injection and 2 days of withdrawal, 2 courses),

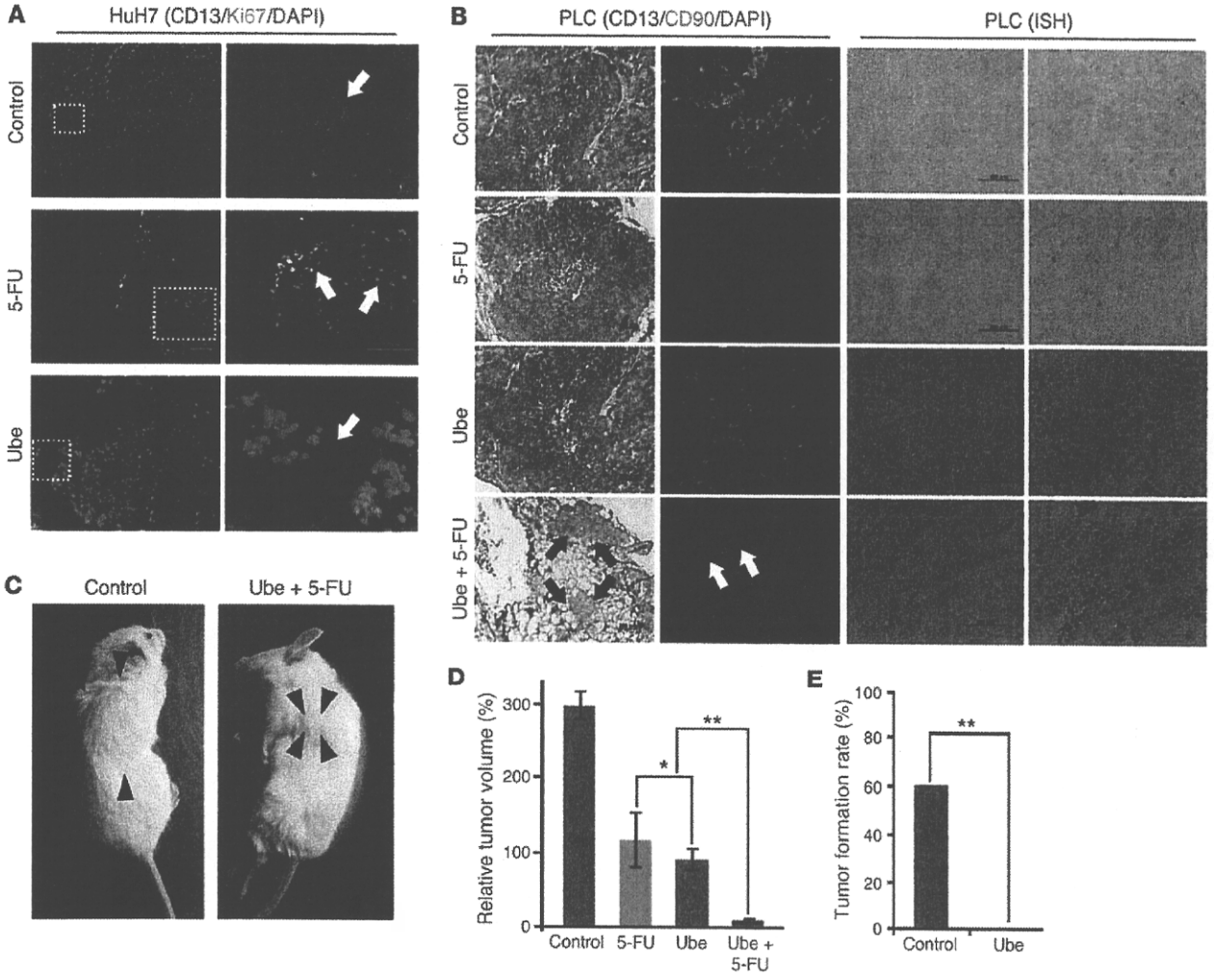

Figure 6

CD13 inhibition elicits cancer regression in vivo. (**A**) HuH7-xenografted mice were treated with 5-FU or ubenimex for 3 days. The sections were stained with anti-human CD13 (red), Ki-67 (green), and DAPI (blue). Each right-hand panel shows a high magnification (×20, control and 5-FU; ×40, Ube) of the white dot square on the left (×10, control and 5-FU; ×20, Ube). White arrows: cellular clusters express CD13 but not Ki-67 (upper panels), residual Ki-67$^+$ cancer cells (middle panels), and a residual CD13$^+$ cell (lower panels). (**B**) PLC/PRF/5-xenografted mice were treated with 5-FU, ubenimex, and ubenimex plus 5-FU for 14 days. The black arrows indicate a small amount of residual cancer. The sections were stained with H&E (×10), anti-human CD13 (red), anti-human CD90 (green), and DAPI (blue) (×20, control, 5-FU, and Ube; ×40, Ube + 5-FU). Nonspecific and fragmented expression of CD13 (white arrow). In situ hybridization for DNA fragmentation (low and high magnification). Black dot-like structures indicate labeled DNA. (**C**) Tumors of control and ubenimex–plus–5-FU–treated mice. Black arrowheads indicate the tumor margin. (**D**) The relative tumor volumes (after treatment [mm^3]/before treatment [mm^3] × 100%) of the control, 5-FU, ubenimex, and ubenimex–plus–5-FU–treated mice. Data represent mean ± SD from independent experiments. *NS; **$P < 0.01$. (**E**) The CD13$^+$ cell–enriched fractions obtained from 5-FU–treated mice were serially transplanted into secondary NOD/SCID mice. The mice were treated with ubenimex (Ube; $n = 6$) or received no treatment (control; $n = 10$) from the day after transplantation for 7 days. Tumor growth was observed for 3 weeks.

most of the CD90$^+$ cells were disrupted and tumors were replaced by a majority of CD13$^+$ cells. After ubenimex treatment (20 mg/kg every day for 14 days), not only were many CD90$^+$ cells present but CD13$^+$ cells were also identified. Interestingly, in cases in which both ubenimex and 5-FU were administered, the majority of tumor cells were disrupted. We identified atypical, nonspecific CD13 expression in these cases (Figure 6B). Taken together with the findings that CD90$^+$ cells produce CD13$^+$ cells within 24 hours and that almost all of the CD13$^+$ cells were disrupted by ubenimex plus 5-FU treatment, the CD13$^+$ cells that appeared in the ubenimex treatment groups may have been newly produced from residual CD90$^+$ cells. Costaining of Ki67 and CD13 revealed that CD13$^+$ cells were negative for the expression of Ki67 (Supplemental Figure 5).

The highly deformed nuclei observed in the ubenimex-plus-5-FU treatment specimens suggested that DNA fragments were present. The DNA fragmentation status was thus assessed by in situ hybridization with terminal deoxynucleotidyl transferase (TdT). There were a few DNA fragments in both the control and 5-FU–treated specimens, whereas there were many more in the ubenimex-treated specimens. Especially in the specimens treated